Journal of Mechanical Engineering Research
http://ojs.bilpublishing.com/index.php/jmer

ARTICLE

# Finite Element Analysis of Stuffing-box Packing Subjected to Thermo-mechanical Loads

**Kaoutar Bahoum*   Mohammed Diany   Mustapha Mabrouki   Jaouad Azouz**
Faculté des Sciences et Techniques, Laboratoire Génie Industriel, Mghila, BP. 535, Beni Mellal, 23000, Morocco

ARTICLE INFO

*Article history:*
Received: 24 October 2018
Accepted: 10 December 2018
Published:28 December 2018

*Keywords:*
Finite element method
Gland stress
Stuffing box
Temperature

ABSTRACT

The principal rule for the stuffing-box packings is to ensure the stem valve sealing. The behavior of these systems is affected by the operating conditions, which are the gland axial stress, the temperature, and the fluid pressure, as well as the mechanical and geometrical properties of the various components. In this paper, a numerical study using finite element method is presented to evaluate the radial contact stresses, the axial stresses, and the lateral pressure coefficients in a stuffing box system under the tightening gland load and the temperature field. The results of the elaborated numerical model show that if the temperature of the confined fluid varies, the contact pressures and the lateral pressure coefficients vary accordingly. When the temperature of the fluid increases, the tightening stress must be adjusted to ensure leak tightness and thus efficiency and efficiency of the gland system.

## 1. Introduction

The packed stuffing boxes are the most systems, designed for sealing, used in the industrial installations. Their role is to ensure sealing of stem-valve, piston pins, and actuators. They stop the fluid confined inside an equipment escape to outside. Braided packing rings, made from deformable and relatively incompressible materials, are compressed to perform this sealing function. The malfunctioning of these assemblies can cause considerable damage to the environment and in some cases life losses. The braided gaskets are compressed by the gland; between the stem and the housing; as shown in Fig.1.

The application of optimum gland axial stress generates contact pressures at packing-housing and at the stem-packing surfaces. The optimum value of this contact pressure is required to ensure the effectiveness and efficiency of the confinement. The confinement of fluid is also, affected during operation by temperature. The transfer of heat from the confined fluid to the components of the assembly has not yet been integrated into the design and modeling of gland assemblies with braided seals.

**Corresponding Author:*
*Kaoutar Bahoum*
*Faculté des Sciences et Techniques, Laboratoire Génie Industriel, Mghila, BP. 535, Beni Mellal, 23000, Morocco*
*Email: bahoum.kaoutar@gmail.com*

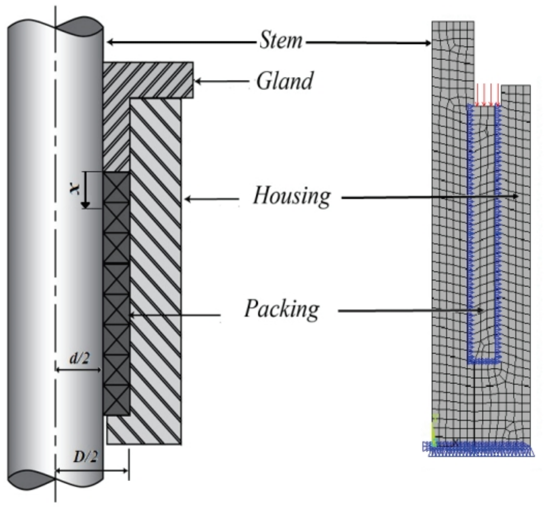


**Figure 1.** A packed stuffing-boxing system

The stresses distribution in stuffing-box systems attracted considerable attention from researchers over the past few decades. During the installation of the stuffing-box systems, the tightening of the gland imposes a non-uniform distribution of the axial pressure along the packing. A substantial portion of this axial stress is transferred to the stem and the housing through the side surfaces of the packing as a contact pressure. Older studies [1] have shown that these stresses vary exponentially according to the axial position as mentioned in the expression in equation (1).

$$\sigma_x=\sigma_D e^{-\beta x}$$
$$q_i=K_i\sigma_D e^{-\beta x} \quad (1)$$
$$q_o=K_o\sigma_D e^{-\beta x}$$

With D the axial stress applied by the gland to the upper packing surface. $q_i$ and qo are radial contact stress at the packing-stem and the packing-housing interfaces. $K_i$ and Ko are the lateral pressure coefficient at the packing-stem and the packing-housing interfaces, which represents the transfer rate of the axial stress in radial stress, and a coefficient characterizing the materials and the geometry of the assembly components.

The first expression of noted$_1$ is proposed by Ochonski [1] considering the equilibrium of forces acting on the packing. The second expression, noted 2, is calculated by Pengym et al[2], adding the balance of moments but always keeping punctual forces. The third expression, noted b$_3$, is proposed by Diany et al.[3], considering a uniform distribution of the contact stresses. Equation (2) presents the three expressions of b.

$$\beta_1=\frac{4(\mu_i K_i d+\mu_o K_o D)}{D^2-d^2}$$

(2)

$$\beta_2=\frac{16(\mu_i K_i d-\mu_o K_o D)}{(D-d)^2}$$

$$\beta_3=\frac{24(\mu_i K_i d-\mu_o K_o D)}{(D-d)^2}$$

Where $d$ and $D$ are the inner and outer packing radii (mm), $\mu_i$ and $\mu_o$ are the Friction coefficient between packing-stem and between packing-housing respectively.

The behavior of the packing in the operating conditions relative to its axial compression, which produces radial contact stresses, is characterized by the factors $K_i$ and $K_o$. The determination of these key factors was initiated experimentally by Bartonicek et al. [4-5], and Klenk et al.[6-7]. Thereafter, Diany et al.[8] proposed a simplified analytical approach using the thick-walled cylinder theory to study stresses and displacements of stuffing-box packing and calculate the lateral pressure coefficients. They proved that the contact pressure ratio is approximately equal to one and that the interface contact pressure depends on different parameters such as the assembly geometry, friction and the mechanical characteristics of the used materials. The same authors [9] developed a hybrid method to characterize the braided packing. Three-axial compression tests combined with finite element simulations were used to evaluate lateral pressure coefficients, elasticity modulus, and Poisson's ratio. They calculated these characteristics for Teflon and flexible graphite packings.

Kazeminia et al. [10-12] presented several analytical models to evaluate the stresses in the stuffing-box components. They presented a contact stress modeling study based on two configurations. The first configuration consists to introduce a variable gap between the packing and the housing in order to create a uniform axial stress distribution. The second configuration consists of inserting one ring of the gasket at a time and using the loading and unloading process to create plastic deformation and residual stresses. They also developed an analytical model based on the combination of ring theory, thin cylinder theory, and beam on elastic foundation theory. The results of the analysis approaches were compared with finite element analysis and experimental tests results.

The temperature influence has not been introduced to date in analytical models. Only a few experimental works have dealt with this influence on stuffing-box packings. Veiga et al. [13] and Girao et al. [14] presented experimental studies; they evaluated the packings expansion under different temperatures and their influence on stresses. These tests show that the packing expansion, due to temperature

  DOI: https://doi.org/ 10.30564/jmer.v1i1.139

variation, increases the applied compressive gland load. The results indicate also that if the volumetric content of packing material is higher, the gland stress increases and the leakage control becomes more difficult.

The purpose of this work is to evaluate the effect of the confined fluid temperature on the distribution of axial stresses, contact pressures, using 2D finite element model of the packed stuffing box. The variation of the lateral contact pressure coefficients is also examined.

## 2. Finite Element Analysis

The study and the modeling of the mechanical assemblies are carried out either by the exploitation of analytical models developed after an accumulated expertise over a long period or by numerical modeling ensured with the help of commercial software more or less sophisticated. A third way is an experimentation either by creating a test bench or by monitoring the actual equipment in the operating sites. In packed stuffing-box case, the study of the temperature effect on mechanical behaviour and leakage is not yet taken into account in the analytical models developed to date. Therefore, a first attempt, using numerical analysis, will certainly allow ground preparation for future analytical studies to consider the temperature effect. In this work, a finite element model, using Ansys software [15], is proposed to evaluate the behaviour of the stuffing box packing assembly subjected to combined loads: clamping force applied by the gland and thermal conditions representing the operating environment.

### 2.1 Finite Element Model

The stuffing-box with hyperelastic packings is composed of four elements: the stem, the packings, the housing and the gland. All components have a cylindrical symmetry. This nature of symmetry, as well as the symmetry of the mechanical load and the boundary conditions reflecting the temperature distribution, allowed working with a simple axisymmetric model in 2D. This axisymmetric model is used to study the combined effect of the fluid temperature and the compression load on the axial distribution of the contact pressure and the lateral pressure coefficients, at the stem-packing and the packing-housing interfaces.

Figure 1 shows this model with the obtained mesh. A2D element with eight nodes, PLANE223, with four degrees of freedom per node (three displacements and temperature), is chosen for this study. The assembly components are in the radial direction contact. Contact elements are used to simulate the reaction of the stuffing-box elements when they are in contact. The elements CONTA172 and TARGE169 are used.

### 2.2 Materials Characteristics

The mechanical properties of the Stuffing-box components affect the resulting stresses and displacements. In this study, the stem and the housing are made of ordinary steel and the braided packing is made of Polytetrafluoroethylene (PTFE). Table 1 shows the mechanical and geometrical properties of the assembly components.

**Table 1.** Stuffing-box components material properties

| | Stem | Packing | Housing |
|---|---|---|---|
| Inner radii (mm) | - | 14.29 | 23.89 |
| Outer radii (mm) | 14.29 | 23.89 | 33.75 |
| Young Modulus (GPa) | 200 | 0.126 | 200 |
| Poison's coefficient | 0.3 | 0.4 | 0.3 |
| Coef. of thermal Exp. $K^{-1}$ | 11.6E-6 | 126E-6 | 11.6E-6 |

### 2.3 Boundary Conditions

The boundary conditions must represent the real operating conditions. Effectively, the upper surface of the packing is subjected to uniform axial compression load representing the clamping load applied by the gland. The lower surfaces of the housing and the stem are at a uniform high temperature transferred from the confined fluid. The other outer surfaces are at room temperature. The radial and axial displacements are blocked at the bottom of the assembly.

The radial contact pressures, the axial stresses and the lateral pressure coefficients under different temperature configurations and tightening load, are examined.

## 3. Results and Discussions

The results of previous studies show that the mechanical and geometrical characteristics of the packed stuffing-box components, as well as the loading conditions, have an influence on the values of the stresses and deformations. To evaluate the effect of the fluid temperature, as a new parameter, on the distribution of stresses and the coefficients characterizing the materials and geometrical proprieties of the assembly components, the axisymmetric model presented in the previous paragraph is implemented. For many axial tightening loads, different values of the fluid temperature have been adopted. The chosen values reflect the actual operating temperature range of the stuffing-box packings.

Figure 2 shows the temperature distribution in the stuffing-box assembly when the fluid temperature is about 250 °C. At the bottom of the housing, the temperature is imposed; it corresponds to the fluid one. The other walls of the system are at room temperature.

More detailed temperature distributions at the inner and outer interfaces of the packing are presented in Figure 3, for three different fluid temperatures. The thermal

 DOI: https://doi.org/ 10.30564/jmer.v1i1.139 

boundary conditions applied to the assembly causes a non-uniform temperature distribution in the two packing interfaces. At the same axial position, the difference in temperature between the two interfaces is greater when the fluid temperature is higher. This difference increases when the axial position is closer to the lower packing surface.

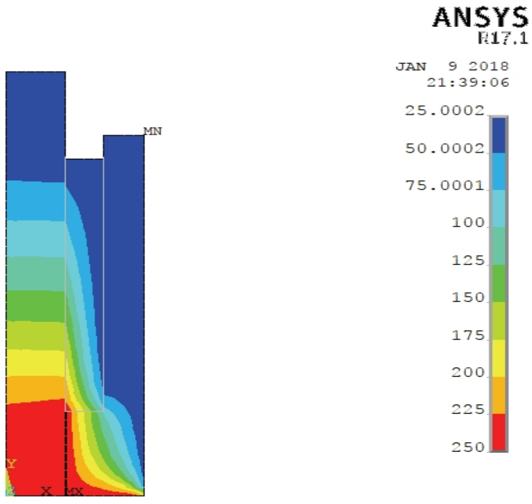


**Figure 2.** Distribution of temperature in stuffing-box packing

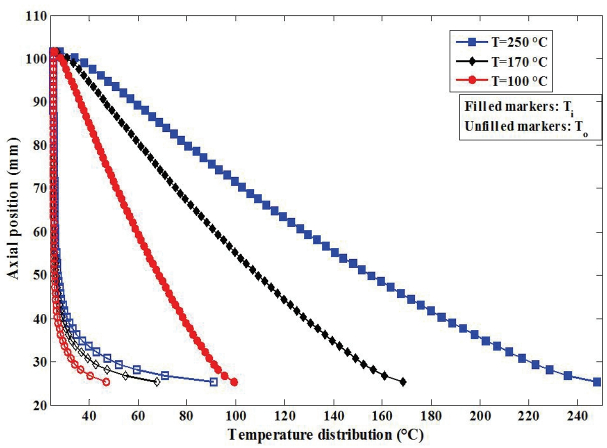


**Figure 3.** Distribution of the temperature in the inner and outer interfaces of the packing

The stuffing box packing ensures the sealing by avoiding the fluid exit towards the external environment. This role is guaranteed by the generation of contact pressures at the stem-packing and packing-housing interfaces. The studies performed at room temperature show that the contact pressures distribution is exponential [1]; this is confirmed in figure 4. Actually, when the temperature imposed everywhere is 25°C, the stresses qi and qo are equals and their values increase when the tightening load increases or when the axial position approaches the packing upper surface.

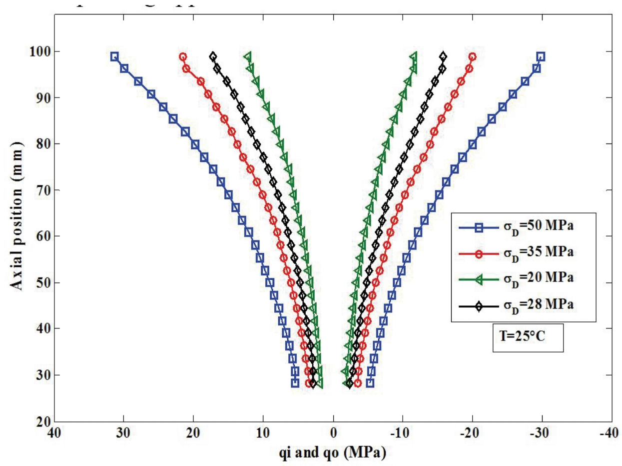


**Figure 4.** Distribution of radial contact stresses at T=25°C

When the fluid temperature is greater than the ambient temperature, the shape of the stress curves moves away from the exponential form. Indeed, in Figure 5 where the fluid temperature is 250°C, the contact pressures have the same value at the bottom packing surface while the clamping force is different.

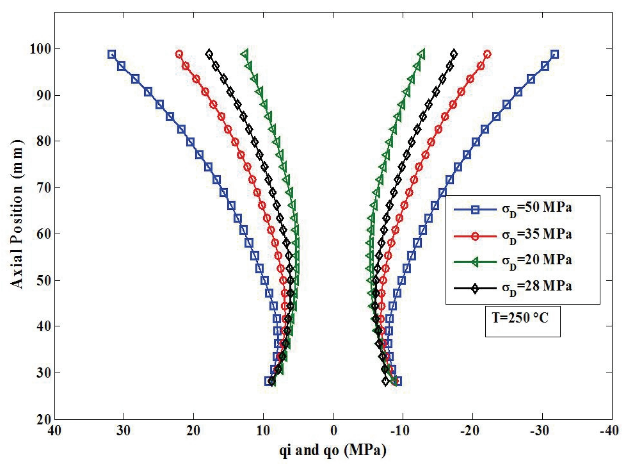


**Figure 5.** Distribution of radial contact stresses at T=250°C

To evaluate the influence of the fluid temperature on the contact pressures, Figure 6 shows the distribution of these stresses for different values of the fluid temperature. The packing upper surface is at the same pressure since it is the same clamping force for all presented cases. The curves corresponding to the different temperatures diverge from an axial position, which depends on the value of the clamping load.

Figure 7. shows the axial stresses distribution at medium diameter of the packing for different temperatures and

  DOI: https://doi.org/ 10.30564/jmer.v1i1.139

gland stress values. The same remarks and conclusions made during the analysis of the other stresses remain valid for these axial stresses.

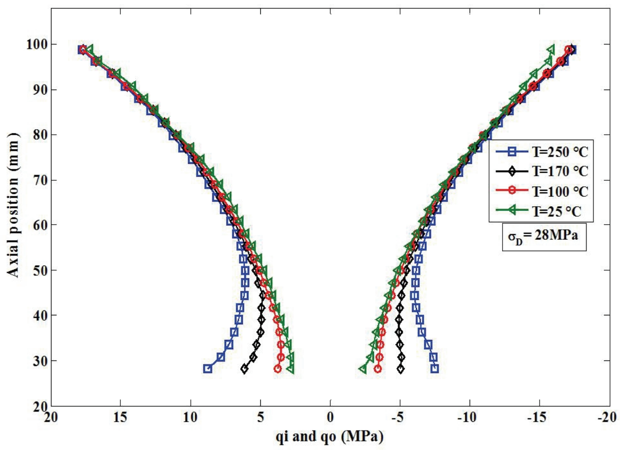


**Figure 6.** Distribution of radial contact stresses for σD= 28 MPa

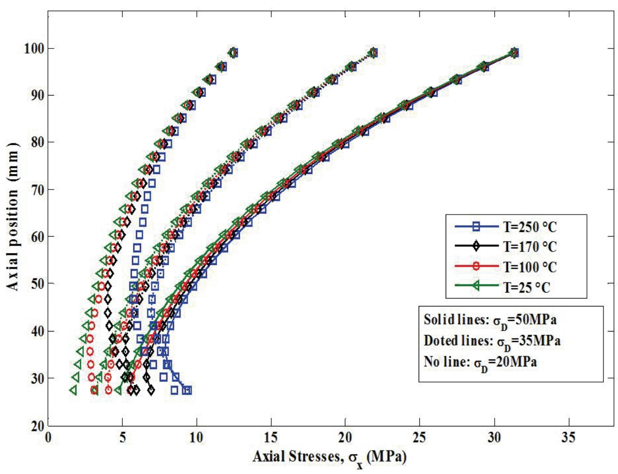


**Figure 7.** Distribution of Axial stresses at the medium diameter of the packing for different temperatures and gland stress values

The stresses expressed in equation (1) are defined by the β coefficient of the exponential form, the clamping load, $\sigma_D$, and the coefficients of lateral pressure, Ki and Ko. The main remark announced during the interpretation of the different curves and the question if the exponential form of the stresses distributions is verified or not. To answer this question, the value of the β coefficient is calculated for all the cases studied and the correspondence rate between the EF curves and the exponential form is by specified. Figure 8 gives the variation of β as a function of the fluid temperature for different clamping loads. Figure 9 shows the compatibility ratio between EF data and equation (1). At room temperature, the β coefficient has the same value for all clamping loads, which confirms the independence of the lateral pressure coefficients of the clamping load at ambient temperature. However, when the fluid temperature is taken into consideration, the value of β changes as a function of temperature and clamping load. In fact, the value of β decreases as the temperature increases or the clamping load decreases. On the other hand, the correspondence rate of the EF curves and equation 1 decreases as the temperature increases or when the clamping load is low. Thus, the exponential shape of the axial distribution of the axial and radial stresses is affected by the fluid temperature consideration. Therefore, it is clear that the lateral pressure coefficients depend on the fluid temperature value and the clamping load.

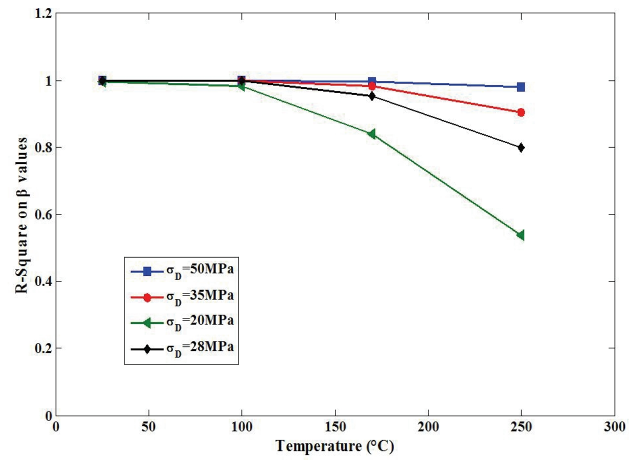


**Figure 8.** Variation of coefficient β as function of the fluid temperature and different gland stress

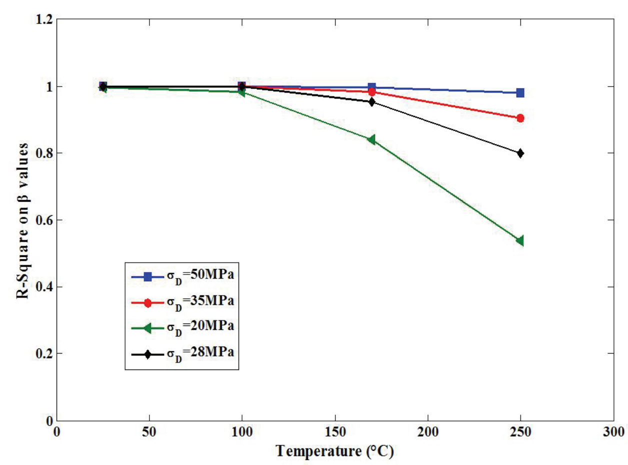


**Figure 9.** Compatibility ratio between EF data and equation (1) as function of the fluid temperature and different gland stress

Figures 10 and 11. show the lateral pressure coefficients at the stem-packing interface, Ki, and at the pack-

 DOI: https://doi.org/ 10.30564/jmer.v1i1.139 

ing-housing interface, Ko, respectively. In an ambient temperature, the shape of the curves is close to the curve theoretically calculated by Diany and Bouzid [8]. When the temperature increases, the value of Ki does not vary significantly and remains around 0.7. On the other hand, Ko changes enormously and even exceeds the unit, which is supposed to be the theoretical maximum value. This last remark obliges us to reconsider the definition of the lateral pressure coefficients to take into account the temperature effect.

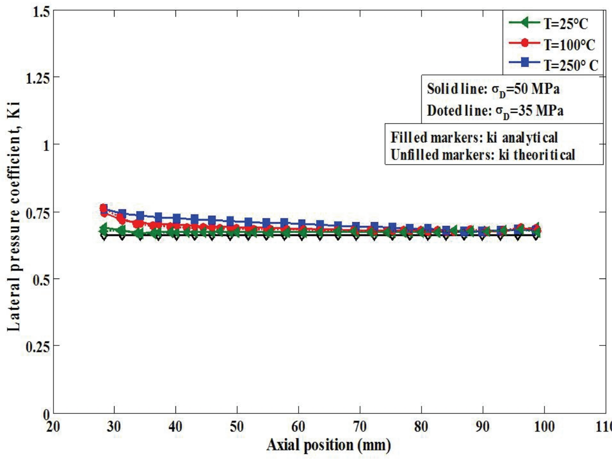


**Figure 10.** Lateral pressure coefficient Ki

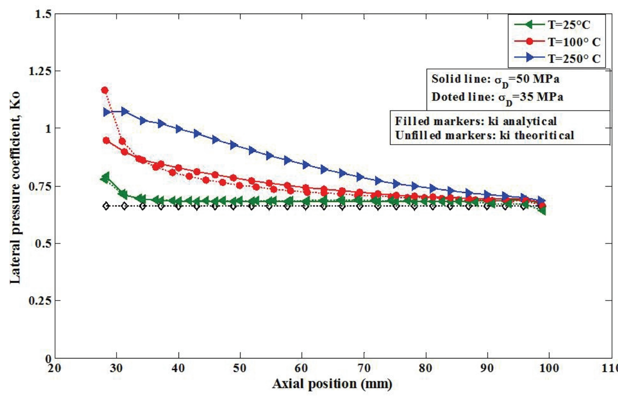


**Figure 11.** Lateral pressure coefficient Ko

## 4. Conclusion

The finite element model of the gland assembly under the combined effect of temperature and tightening load is presented. The results of this elaborated numerical model show that:

The variation of the temperature of the confined fluid influences the contact pressures and the axial stresses distributions. Indeed, for the ambient temperature, the stresses shapes respect the equation (1), and when the temperature increases, the curves move away from the exponential form expected in theoretical studies.

The definition of the lateral pressure coefficients should be reconsidered to take into account the temperature effect.

The tightening load must be adjusted when the fluid temperature increases in order to ensure leak tightness and the efficiency of the system.

All these finite element analysis conclusions must be compared and validated with analytical and experimental studies.

Nomenclature:

$\sigma_x$ : Axial stress distribution in the packing, (MPa)

$\sigma_D$: Gland axial stress (MPa)

$X$: Axial position (MPa)

$k_{i,}$ $k_o$: Lateral pressure coefficient between packing-stem and between packing-housing respectively

$\mu_{i,}$ $\mu_o$ : Friction coefficient between packing-stem and between packing-housing respectively

$q_{i,}$ $q_o$: Radial contact stress at the packing-stem interface and at the packing-housing interface respectively (MPa)

$d$, $D$ : The inner and outer packing radii (mm)

$\mu i$, $\mu o$ : The Friction coefficient between packing-stem and between packing-housing respectively.

$T$ : Celsius temperature scale

### References

[1] Ochonski, W., "Radial Stress Distribution and Friction Forces an a Soft-Packed Stuffing-Box Seal," Tribology International, 1988, 21(1), 31-38.

[2] Pengyun S., Kuangmin C. and Zongyun D., "A Theoretical Analysis of the Lateral Pressure in a Soft Packed Stuffing Box Seal," Tribology International, 1997, 30(10), 759-765.

[3] Diany, M. and Bouzid, A,-H. Evaluation of contact stress in stuffing box packing. In: 2006 ASME-PVP conference, paper no. PVP2006-ICPVT11-93083, Vancouver, Britisg Columbia, 2006.

[4] Bartonicek, J., and Schoeckle, F., "Approach to a Correct Function of Stuffing Boxes," 1996 Computer Technology: Applications and Methodology, ASME, New York,1996, 326, 115–121.

[5] Bartonicek, J., and Schoeckle, F., "Tightness and Accurate Mounting of Bolted Joints," 1996 Computer Technology: Applications and Methodology, ASME, New York, 1996, 326, 171–178.

[6] Klenk, T., Kockelmann, H., Roos, E., Bartonicek, J., and Schoeckle, F., "Characteristics and Testing Techniques for Stuffing Box Packings," ASME Pressure Vessels and Piping Conference,1999, 382, 135–143.

[7] Klenk, T., Kockelmann, H., Hahn, R., and Roos, E., "High Grade Proof for Gaskets According to TA-Luft and VDI 2440," ASME Pressure Vessels and Piping Division Conference, 2001, 416, 163–167.

  DOI: https://doi.org/ 10.30564/jmer.v1i1.139

[ 8 ] Diany, M., and Bouzid, A., "Analytical Evaluation of Stresses and Displacements of Stuffing-Box Packing Based of Flexibility Analysis," Tribol. Int., 2009, 42 (6), 980–986.

[ 9 ] Diany, M. and Bouzid, A,-H. An Experimental– Numerical Procedure for Stuffing Box Packing Characterization and Leak Tests. ASME Journal of Tribology, 2011, 133(1).

[10] Kazeminia, M. and Bouzid, A.-H. Analysis of stresses and strains in packed stuffing-boxes. In: Proceedings of the ASME Pressure Vessels and Piping Conference (PVP '14), Anaheim, Calif, USA, 2014, 1–11.

[11] Kazeminia, M. and Bouzid, A.-H. Analytical and numerical evaluation of the axial stress distribution of two soft-packed stuffing-box configurations. In: Proceedings of the ASME Turbo Expo 2014, Turbine Technical Conference and Exposition, D¨usseldorf, Germany, 2014, 1–8.

[12] Kazeminia, M. and Bouzid, A.-H. Stress analysis of packed stuffing-boxes. Journal of Pressure Vessel Technology, 2015, 137, 5.

[13] Veiga, J. C., Carmo, A. S. and Girao, C. D. The influence on the stuffing box of the forces generated by packing thermal expansion. In: Proceedings of the Pressure Vessels Piping Division Conference (ASME '11), Baltimore, Md, USA, 2011, 227–233.

[14] Girao, C. D. and Guenther, K. Evaluation of stuffing box forces associated with the thermal expansion of e-PTFE and graphite packing sets. In: Proceedings of the ASME Pressure Vessels and Piping Conference, Toronto, Canada, 2012, 167173.

[15 Ansys. Standard Manuel. Version 17.1.